Food Control

Prediction of olive ripening degree combining image analysis and FT-NIR spectroscopy for virgin olive oil optimisation

--Manuscript Draft--

Manuscript Number:	FOODCONT-D-20-03424R1
Article Type:	Research Paper
Keywords:	olive quality; maturity index; intact fruit; image analysis; near infrared spectroscopy
Corresponding Author:	Silvia Grassi, Ph.D. Università degli Studi di Milano Milano, ITALY
First Author:	Cristina Alamprese
Order of Authors:	Cristina Alamprese
	Silvia Grassi, Ph.D.
	Alessio Tugnolo
	Ernestina Casiraghi
Abstract:	This work proposes classification models for the prediction of olive maturity index based on Fourier Transform-Near Infrared (FT-NIR) spectra of intact drupes. An image analysis (IA) method was purposely developed for the objective evaluation of the maturity index. Thirteen cultivars at different ripening stages were harvested along three years. The reliability of the IA method was confirmed by the highly significant correlation with the common visual evaluation of maturity index. Classification models were developed with Partial Least Square-Discriminant Analysis (PLS-DA), using IA results and FT-NIR spectra of olives collected in diffuse reflectance. Most PLS-DA models calculated separately for olive origin gave sensitivity and specificity values in prediction higher than 81%. The global model performed slightly worse (sensitivity, 79%; specificity, 75%), but it is definitely more robust and can provide the olive sector with a fast, green and non-destructive olive sorting method for the production of high quality virgin oil.

Prediction of olive ripening degree combining image analysis and FT-NIR spectroscopy for virgin olive oil optimisation

Cristina Alamprese[1], Silvia Grassi[1*], Alessio Tugnolo[2], Ernestina Casiraghi[1]

[1]Department of Food, Environmental, and Nutritional Sciences (DeFENS), Università degli Studi di Milano, via G. Celoria 2, 20133 Milan, Italy

[2]Department of Agricultural and Environmental Sciences (DiSAA), Università degli Studi di Milano, via G. Celoria 2, 20133 Milan, Italy.

* Corresponding author; e-mail address: silvia.grassi@unimi.it

Abstract

This work proposes classification models for the prediction of olive maturity index based on Fourier Transform-Near Infrared (FT-NIR) spectra of intact drupes. An image analysis (IA) method was purposely developed for the objective evaluation of the maturity index. Thirteen cultivars at different ripening stages were harvested along three years. The reliability of the IA method was confirmed by the highly significant correlation with the common visual evaluation of maturity index. Classification models were developed with Partial Least Square-Discriminant Analysis (PLS-DA), using IA results and FT-NIR spectra of olives collected in diffuse reflectance. Most PLS-DA models calculated separately for olive origin gave sensitivity and specificity values in prediction higher than 81%. The global model performed slightly worse (sensitivity, 79%; specificity, 75%), but it is definitely more robust and can provide the olive sector with a fast, green and non-destructive olive sorting method for the production of high quality virgin oil.

Keywords: olive quality; maturity index; intact fruit; image analysis; near infrared spectroscopy.

Abbreviations

AR, Abruzzo Region; CA, Calabria Region; CV, cross-validation; EVOO, extra virgin olive oil; FN, false negative; FP, false positive; FT-NIR, Fourier Transform-Near Infrared; IA, image analysis; LV, Latent Variable; NIR, Near Infrared; MI, Maturity Index; PC, Principal Component; PCA, Principal Component Analysis; PLS-DA, Partial Least Square-Discriminant Analysis; PR, Apulia Region; ROI, Region of Interest; SCI, Surface Colorimetric Index; SENS, sensitivity; SPEC, specificity; SR, Sardinia Region; SNV, Standard Normal Variate; TP, true positive; TN, true negative.

1. Introduction

The quality of virgin and extra virgin olive oils is strongly related to the physiological conditions and the ripening stage of the fruits from which they are extracted. In general, a progressive deterioration of oil quality is observed as fruit ripening progresses, but different behaviours have been registered in distinct olive cultivars (Camposeo et al., 2013; Garcia et al., 1996). To date, the optimal harvest time has been selected mainly using traditional approaches and personnel experience rather than scientific criteria (Garcia et al., 1996), thus making difficult the objective optimisation of the oil quality. The most common method used to define the optimal harvest time is based on olive visual inspection (Uceda and Frias, 1975), but other evaluations have been proposed over the years, such as the measurement of fruit detachment force and fresh weight (Camposeo et al., 2013), the determination of flesh firmness (Garcia et al., 1996) or respiration rate (Ranalli et al., 1998), as well as the drupe oil (Allalout et al., 2011; Correa et al., 2019) and polyphenol (Morelló et al., 2004) content. However, all these methods are laborious and time-consuming, thus limiting the efficiency of controls and preventing the possibility to develop in-line applications for the olive oil industries.

In order to overcome these issues and develop rapid, reliable and automatic methods for the assessment of olive ripening stage, computer vision and near infrared (NIR) spectroscopy approaches have been recently studied. For instance, Guzmán et al. (2015) proposed a machine vision system based on the use of infrared and visible images for the prediction of maturity index of Picual olives determined by a panel of experienced evaluators. Soto et al. (2018) presented a proposal to automatically determine olive oil quality parameters by processing images acquired from olive fruits. They tested 84 batches of olives and the image processing was guided by experts' assessment of fruit

conditions. Ram et al. (2010) applied image processing to the prediction of oil quantity in Picual and Souri olives during the ripening season. As for vibrational spectroscopy, Gracia and León (2011) studied the evolution of oil and moisture content in intact olives during the maturity process by using a portable NIR device and testing eight Spanish cultivars. Cayuela and Camino (2010) carried out a similar study, testing the usefulness of a portable Vis/NIR spectrometer for the prediction of fruit moisture, oil content, fruit maturity index and oil free acidity of two Spanish olive varieties. Bellincontro et al. (2012) applied a portable NIR-AOTF (Acousto Optically Tunable Filter) device for the prediction of the main phenolic compounds (oleuropein, verbascoside, and 3, 4-DHPEA-EDA) and total phenols of three Italian olive cultivars. All these studies investigated the quality parameters by collecting spectra on the single fruits and considering only one harvest season. Salguero-Chaparro et al. (2013) analysed 250 samples of intact olives belonging to fifty varieties and harvested in two crop seasons in order to test a NIR device set on a conveyor belt for the on-line determination of the oil content, moisture and free acidity. Other similar works were reviewed by Stella et al. (2015), who concluded that the advantages of NIR spectroscopy over traditional analytical methods are clear, but the robustness of the developed models is affected by small datasets. Similarly, Nenadis and Tsimidou (2017) reviewed papers focused on vibrational techniques addressing quality and authenticity issues of olives and virgin olive oils and they discussed the need for validation guidelines and open-access spectral databanks in order to standardize these techniques and use them in the official control. They also pointed out the importance of the reference analytical methods for the successful calibration of chemometric models and the reduction of errors. In this respect, the use of visual inspection evaluations as references for the calibration of olive

classification models based on maturity index can represent a source of errors preventing the development of reliable methods.

Thus, the aim of this work was the development of a classification model based on Fourier Transform-Near Infrared (FT-NIR) spectra of aliquots of intact olives using as *a priori* information the olive maturity index objectively evaluated through an image analysis method purposely developed. A big dataset was used to set up the proposed methodology, considering thirteen Italian olive cultivars at different ripening stages, harvested during three crop seasons (from 2016 to 2018), for a total of 303 samples corresponding to as many olive aliquots.

2. Materials and Methods

2.1. Experimental plan

Olives at different maturity stages were collected from September to December over three harvesting years (2016, 2017, and 2018). Thirteen cultivars typical of four different Italian regions were sampled as detailed in Table 1.

<Table 1>

For each sampling time (from T1 up to T5) and cultivar, three sample units (500 g each) were collected from different labelled trees of the same grove. The Maturity Index (MI) was evaluated picking olives from the three sample units; furthermore, two aliquots (100 g each) were withdrawn from each sample unit, to be used for surface colorimetric index assessment, image analysis, and FT-NIR spectroscopy. A total of 303 aliquots of olives in adequate hygienic and qualitative conditions were analysed after wiping olive surface with paper towel.

2.2. Visual assessment of ripening stage

96 *2.2.1. Maturity Index*

97 From each olive sample unit, 100 drupes were randomly collected to assess the MI
98 according to the visual approach proposed by Uceda and Frias (1975). The method
99 classifies olives in eight classes according to both skin and pulp colour and then MI is
100 calculated following equation (1):

101 $$MI = \frac{1}{N} \sum_{i=0}^{7} (i \times n_i) \quad (1)$$

102 where *i* is the class number, *ni* is the number of olives belonging to the i class, and *N* is
103 the total number of considered olives (100).

104 *2.2.2. Surface Colorimetric Index*

105 Each olive aliquot was evaluated by a non-destructive visual assessment of the ripening
106 stage, considering only the skin colour as reported in Table 2.

107 <Table 2>

108 Results were expressed by an index referred as Surface Colorimetric Index (SCI)
109 calculated according to equation (2):

110 $$SCI = \frac{1}{N} \sum_{i=1}^{4} (i \times n_i) \quad (2)$$

111 where *i* is the class number, n_i is the number of olives belonging to the i class, and *N* is
112 the total number of considered olives (60).

113 *2.3. Image analysis*

114 Images of each olive aliquot were collected using a flatbed scanner (Scanjet 8300, HP
115 Inc., Palo Alto, CA, USA) controlled by VueScan software (v. 9.4, 2016, Hamrick
116 Software, Sunny Isles Beach, FL, USA). The entire aliquot was placed on the scanner
117 glass and covered with a black box to prevent light losses and avoid noise from the
118 environment. Two images were acquired for each aliquot, at 600 dpi resolution, with a

24 bit colour depth and saved in TIFF format; the olives were blended in-between the two acquisitions.

Images were then elaborated using a Matlab (v. 2016a, Mathworks, Inc., Natick, MA, USA) routine purposely developed to objectively assess the olive ripening stage. At first, in order to distinguish olives from background, a Region of Interest (ROI) was segmented applying the Superpixel algorithm on each RGB channel. The algorithm performs a simple linear iterative clustering (Achanta et al., 2012) in order to group pixels into regions with similar intensity values. From a practical point of view, this algorithm groups together neighbour pixels based on their RGB intensity values and allows the background removal. An example of the original image and the segmented one is reported in Fig. 1.

<Figure 1>

The average red channel intensity of the segmented mask, containing only the olive pixels, was then calculated and used to assign each olive aliquot to a maturity class (named IA).

2.4. FT-NIR spectroscopy

Each olive aliquot was placed in a glass Petri dish and analysed in diffuse reflectance by a FT-NIR spectrometer (MPA, Bruker Optics, Milan, Italy) equipped with an integrating sphere (Fig. 2). Spectra were collected in the whole NIR region (12500 – 4000 cm^{-1}), with a resolution of 8 cm^{-1} and 32 scans for both sample and background. Two spectra were collected for each aliquot, blending the olives in-between measurements.

<Figure 2>

142 *2.5. Data analysis*

143 Linear correlations between the maturity class indices (i.e. MI *vs* SCI and SCI *vs* IA)
144 were evaluated calculating Pearson correlation coefficients and the corresponding
145 significance (p-value).

146 The two FT-NIR spectra collected from each olive aliquot were averaged and organised
147 in a global dataset. Furthermore, four independent datasets were created according to
148 olive origin (AR, CR, PR, and SR). Spectra were reduced in the 10500 - 4000 cm^{-1}
149 range and pre-treated with smoothing, Standard Normal Variate (SNV), and first
150 derivative, alone or in combination. Before further analyses, spectral data were explored
151 by Principal Component Analysis (PCA). Then, the maturity classes identified by image
152 analysis were used as *a priori* information for the development of classification models
153 based on Partial Least Square-Discriminant Analysis (PLS-DA). A dataset (206
154 samples) constructed with aliquots of olives collected in 2017 was used for model
155 calibration and cross-validation (venetian blinds, ten splits). A test set for external
156 validation was created merging data collected during 2016 and 2018 (97 aliquots). The
157 PLS-DA model performance was evaluated by comparing the reference class of each
158 sample (IA) with the class predicted by the model. The most probable approach was
159 applied to assign samples to classes. Samples were assigned to the class reaching the
160 highest probability regardless the probability magnitude, thus no probability threshold
161 was considered. This approach is advantageous if there is the need of unambiguous
162 class assignment when "no class" o “multiple class” has no meaning. Sensitivity and
163 specificity were calculated for each maturity class in calibration, cross-validation and
164 prediction. Sensitivity (*SENS*, equation 3) expresses the model capability to correctly
165 recognize samples belonging to the considered class. Specificity (*SPEC*, equation 4)

describes the model capability to correctly reject samples that do not belong to the considered class (Ballabio and Consonni, 2013).

$$SENS = \frac{TP}{(TP+FN)} * 100 \quad (3)$$

$$SPEC = \frac{TN}{(TN+FP)} * 100 \quad (4)$$

where TP are the true positive samples, FN are the false negative samples, TN are the true negative samples, and FP are the false positive samples.

Both SENS and SPEC can assume values between 0% and 100%, being 100% the totally correct classification of TP and the totally correct rejection of TN for sensitivity and specificity, respectively.

All data analyses were performed in Matlab environment (v. 2016a, Mathworks, Inc., Natick, MA, USA), using the PLS toolbox (v. 8.5, Eigenvector Research, Inc., Aeattle, WA, USA).

3. Results and discussion

3.1. Objective assessment of olive maturity class by image analysis

MI of olive samples ranged from 0 to 5.9, with a total mean of 2.4 and a standard deviation value of 1.4. The highest mean values (3.0-3.3) were reached by the cultivars Filogaso (CR), Corsicana (SR), Sivigliana (SR), and Dritta (AR), while the cultivar Semidana (SR) had an average MI lower than 1.0. Thus, despite the long harvesting period considered (about 4 months), none of the olive cultivars reached the highest possible value of MI (7.0). This is in agreement with results of previous published works, in which MI ranged from 0 to 6 (Baccouri et al., 2007) or from 0 to 3 (Vidal et al., 2019), depending on the considered olive cultivars. In general, it has been reported

189 that the best results in terms of both oil quantity and quality (mill extraction yield,
190 induction time, polyphenol content, aromatic compounds, sensory score) are obtained
191 with olives harvested when their degreening is limited to the skin, i.e. with a maturity
192 index less than 4 in a 0-7 scale (Camposeo et al., 2013).
193 The MI assessment is very time-consuming and the obtained results strongly depend on
194 the experience of the evaluator, the olive health and physical state, and the
195 environmental conditions, such as lighting (Guzmán et al., 2015). Due to these issues, a
196 simpler and non-destructive visual evaluation based only on skin colour was also
197 performed on all the olive samples. The resulting SCI ranged from 1 to 4, with a total
198 mean of 2.3 and a standard deviation value of 1.0. MI and SCI values resulted highly
199 correlated ($r = 0.95$; $p < 0.001$), thus indicating the effectiveness of the procedure
200 developed for SCI assessment, and the higher importance of the skin colour with respect
201 to the pulp one. However, also the SCI determination is highly dependent on analysis
202 conditions and evaluator experience, whereas a vision system approach could overcome
203 these drawbacks. In fact, the scanning procedure allows lighting standardisation, and
204 image analysis gives more objective and reproducible results. Thus, a suitable image
205 analysis procedure was developed and the average value of the red channel was used to
206 assign the olive aliquots to a maturity class.
207 A simpler method, based on three-class maturity assignment, as reported in Table 3,
208 was considered instead of the four-class division of SCI. A global red channel
209 thresholding was defined by considering the images of all the olive cultivars and
210 sampling times of the crop seasons 2016 and 2018. The reliability of the thresholding
211 was assessed on the images acquired in 2017.
212 <Table 3>

The IA index had a global mean of 2, with a standard deviation value of 1. Also in this case, a highly significant correlation was found between IA and SCI values ($r = 0.85$, $p < 0.001$), thus demonstrating that the subjective visual inspection can be substituted by the objective vision system approach, enabling the standardisation and automation of the maturity index evaluation. Furthermore, samples of the Interquartile Range (IQR) of the three IA classes had MI ranges of 0.80 - 1.55, 1.65 - 3.00, and 3.40 - 4.55, for class 1, 2, and 3, respectively, thus demonstrating the reliability of the IA method in discriminating olives with different ripening degree.

3.2. Interpretation of olive FT-NIR spectra

The raw spectra acquired for each aliquot of olives are reported in Fig. 3a. In the region between 9000 and 8000 cm^{-1} it is possible to notice the characteristic bands mainly linked to the absorption of fats and oils (Correa et al., 2019). Indeed, the absorbance at 8733 and 8620 cm^{-1} is related to the stretching of the C–O bonds of aliphatic esters, while the second overtone of C–H stretching vibrations of alkyl groups and alkenes occurs at 8245 and 8030 cm^{-1} (Fernández-Espinosa, 2016). Other characteristic bands are present around 6900 cm^{-1} (6842 cm^{-1}, $–CH_2–$ 2C–H stretch + C–H deformation; 6900 cm^{-1}, first overtone of -OH bond) and in the region between 6700 and 5300 cm^{-1}, characterised by CH_3-CH stretch (5950 cm^{-1}) and OH, -CO stretch (5500 cm^{-1}). The absorbance around 5200 cm^{-1} is related to the harmonic and combination bands of O–H bonds in hydroxyl groups (Fernández-Espinosa, 2016; Trapani et al., 2017). Besides, the relevant differences in absorbance intensity within 4500 and 4000 cm^{-1} are linked to the combination of CH stretching with other vibrational modes (Casale and Simonetti, 2014). The peak at 4085 cm^{-1} was characteristic of the olives assigned to the IA classes 1 (100% green skin colour) and 2 (<50% of the skin colour turning red). Actually, this

peak disappeared with the ripening progress, being replaced in the spectra of the class 3 olives by two peaks at 4335 cm^{-1} (CH second overtone) and 4262 cm^{-1} (CH_2 second overtone) (Trapani et al., 2017).

<Figure 3>

Due to its scarce relevance, the region between 12500 and 10500 cm^{-1} was removed before further analyses and the spectra were pre-treated with smoothing (Savitzky–Golay, zero polynomial order, 15 points) and first derivative (Savitzky–Golay, second polynomial order, 15 points) to enhance differences (Fig. 3b). The pre-treated spectra collected from olive samples of the IA class 3 better highlighted the changes occurring with the olive ripening. In particular, the higher absorbance in the region 8600 - 8330 cm^{-1} and at 5800 cm^{-1} and the lower intensity in the 8350 - 8000 and 5850 - 5580 cm^{-1} ranges of the completely ripe drupes (class 3) are linked to the higher oil content with respect to the less ripe fruits (Hernández-Sánchez and Gómez-del-Campo, 2018).

3.3. Qualitative inspection of spectral data

The observed differences in spectra of olive samples were investigated by performing a PCA. The better differentiation among IA classes was observed for the spectra transformed by smoothing and first derivative. Sample distribution along the first two PCs (around 80% of the explained variance) was marked according to the maturity stage (Fig. 4a) and origin (Fig. 4b).

<Figure 4>

The green skin drupes (IA class 1) generally had positive PC1 and PC2 values, whereas IA class 3 samples were characterised by negative PC1 scores (Fig. 4a). Accordingly, the samples with an intermediate ripening stage (IA class 2) were distributed in-between the other two classes.

By the loading inspection it was possible to associate samples with positive PC1 scores, i.e. drupes with green skin colour, to higher absorbance at 6900 cm^{-1} (first overtone of -OH bond), 5850 - 5580 cm^{-1} (OH stretch, -CO stretch), and 4500 - 4000 cm^{-1} (Fig. 4c). Sample distinction based on olive origin (Fig. 4b) was not clear, remarking that the main differences among the olives were related to the maturation progress, rather than the growing area or the cultivar. Similarly, Fernández-Espinosa (2016) reported difficulties in discriminating olive varieties using AOTF-NIR spectra.

The data exploration did the groundwork for the development of a classification model able to discriminate olives according to the maturity class identified by image analysis.

3.4. FT-NIR spectroscopy for the assessment of olive maturity class

Olive classification models based on IA maturity classes were developed applying the PLS-DA algorithm, based on the optimisation of covariance between *X* and *Y*, substituting the *Y* with a dummy variable having three levels, i.e. the number of IA classes. After the regression procedure, the *y* predicted values for each sample were translated into class membership (classification procedure). The class assignation was then performed based on probability, in a way that each sample was assigned to the class that had the highest probability regardless of the magnitude of the probability (Ballabio and Consonni, 2013). The performance of the global model (based on data of all the olive samples) and the origin models (one model for each region of provenance of the olives) was evaluated in terms of SENS and SPEC in calibration, cross-validation and prediction (Table 4).

<Table 4>

Different spectral pre-treatments were evaluated for the classification model development; the best performance was achieved when spectra were transformed by

285 smoothing and first derivative. SENS and SPEC average values in prediction for the
286 global model were 79% and 75%, respectively, being mainly affected by the high SENS
287 value of classes 1 and 3 (>85%) and the low SENS and SPEC values of class 2 (64%
288 and 72%, respectively). This means that samples with MI values from 0.80 to 1.55 (the
289 IQR for class 1) were correctly classified with a SENS of 85%, similarly to samples
290 with MI values from 3.40 to 4.55 (the IQR for class 3). The higher misclassification of
291 the intermediate class was expected as the maturation steps are not circumscribable, but
292 they are the result of continuous modifications along the biological process. The
293 misclassification is also justified by the high variability of samples present in class 2.
294 Indeed, the IQR of class 2 includes samples with a larger range of MI (from 1.65 to
295 3.00), and 10.7% of the samples included in this class (9 samples out of 84) has MI
296 values outside the IQR range.
297 Due to the limited number of papers focused on the prediction of olive maturity stages
298 by NIR spectroscopy, a comparison with previously published data is difficult, also
299 because of the different chemometric models and performance figures used. For
300 instance, the work by Cayuela and Camino (2010) assessed the olive MI using Vis-NIR
301 data, but a PLS regression model was applied. They obtained a root mean square error
302 of prediction (RMSEP) of 0.51 with a 1-6 MI range, i.e. a RMSEP% of 15.7, that was
303 considered a good performance being the reference method susceptible of a large error.
304 Even though the PCA demonstrated that there was not a clear distribution of samples
305 based on olive origin, PLS-DA models for each region of provenance were in any case
306 developed to assess if a better performance could be achieved. This was the case of AR,
307 CR and PR models, being SENS and SPEC in prediction higher than 82% and 81%,
308 respectively. On the contrary, the SR model reached values of SENS and SPEC in

prediction of 75% and 69%, respectively, lower than the figures of merit of the global model. The lower performance of the SR model could be ascribed to the lowest number of samples used to calibrate (43) and validate the model (20), which could lead to a model less stable, also considering the lower range of MI variability of the Semidana olives belonging to this dataset.

Notwithstanding the slightly worse performance of the global model with respect to most of the origin-based ones, it should be considered that it is definitely more robust being constructed on a dataset of 303 samples, i.e. aliquots of olives belonging to thirteen different cultivars harvested over three years. Thus, the global model could be used on a larger scale, no matter the olive cultivar or origin.

4. Conclusions

In conclusion, the work proposes FT-NIR classification models for the objective evaluation of olive ripening stage based on maturity classes objectively assessed by an image analysis method. The developed methodology is easy, green and non-destructive and it overcomes the issues of the visual evaluations commonly applied in the olive sector. Moreover, the use of IA results for the calibration of classification models make them highly reliable, reducing the magnitude of the possible errors. Such a tool can be used for sorting olives directly at the entrance in the mill or even in field - if transferred in a portable device – thus providing olive growers and oil producers with an important decision-making support for the optimisation of virgin and extra virgin olive oil, with a major economic potential for all the olive oil chain. Moreover, it has to be pointed out that the implementation of NIR systems do the groundwork for the prediction of olive and oil quality parameters, thus justifying the use of spectroscopy over the IA used for the calibration step.

Declaration of interest

The Authors declare no conflicts of interest.

Funding sources

This work was supported by AGER 2 Project, grant no. 2016-0105.

References

Achanta, R., Shaji, A., Smith, K., Lucchi, A., Fua, P., and Süsstrunk, S. (2012). SLIC superpixels compared to state-of-the-art superpixel methods. *IEEE Transactions on Pattern Analysis and Machine Intelligence*, 34(11), 2274-2282.

Allalout, A., Krichene, D., Methenni, K., Taamalli, A., Daoud, D., and Zarrouk, M. (2011). Behaviour of super-intensive Spanish and Greek olive cultivars grown in Northern Tunisia. *Journal of Food Biochemistry*, 35, 27–43.

Baccouri, B., Zarrouk, W., Krichene, D., Nouairi, I., Youssef, N.B., Daoud, D., and Zarrouk, M. (2007). Influence of fruit ripening and crop yield on chemical properties of virgin olive oils from seven selected oleasters (*Olea europea* L.). *Journal of Agronomy*, 6, 388-396.

Ballabio, D., and Consonni, V. (2013). Classification tools in chemistry. Part 1: linear models. PLS-DA. *Analytical Methods*, 5, 3790-3798.

Bellincontro, A., Taticchi, A., Servili, M., Esposto, S., Farinelli, D., and Mencarelli, F. (2012). Feasible application of a portable NIR-AOTF tool for on-field prediction of phenolic compounds during the ripening of olives for oil production. *Journal of Agricultural and Food Chemistry*, 60, 2665−2673.

355 Camposeo, S., Vivaldi, G.A., and Gattullo, C.E. (2013). Ripening indices and
356 harvesting times of different olive cultivars for continuous harvest. *Scientia*
357 *Horticulturae*, 151, 1–10.
358 Cayuela, J.A., and Camino, M.D.C.P. (2010). Prediction of quality of intact olives by
359 near infrared spectroscopy. *European Journal of Lipid Science and Technology*,
360 112(11), 1209-1217.
361 Casale, M., and Simonetti, R. (2014). Near infrared spectroscopy for analysing olive
362 oils. *Journal of Near Infrared Spectroscopy*, 22, 59-80.
363 Correa, E.C., Roger, J.M., Lleó, L., Hernández-Sánchez, N., Barreiro, P., and Diezma,
364 B. (2019). Optimal management of oil content variability in olive mill batches by NIR
365 spectroscopy. *Scientific Reports*, 9, 1-11.
366 Fernández-Espinosa, A.J. (2016). Combining PLS regression with portable NIR
367 spectroscopy to on-line monitor quality parameters in intact olives for determining
368 optimal harvesting time. *Talanta*, 148, 216-228.
369 Garcia, J.M., Seller, S., Pérez-Camino, M.C. (1996). Influence of fruit ripening on olive
370 oil quality. *Journal of Agricultural and Food Chemistry*, 44, 3516-3520.
371 Gracia, A., and León, L. (2011). Non-destructive assessment of olive fruit ripening by
372 portable near infrared spectroscopy. *Grasas y Aceites*, 62(3), 268-274.
373 Guzmán, E., Baeten, V., Fernández Pierna, J.A., and García-Mes, J.A. (2015).
374 Determination of the olive maturity index of intact fruits using image analysis. *Journal*
375 *Food Science and Technology*, 52, 1462-1470.
376 Hernández-Sánchez, N., and Gómez-del-Campo, M. (2018). From NIR spectra to
377 singular wavelengths for the estimation of the oil and water contents in olive fruits.
378 *Grasas y Aceites*, 69(4), e278.

379 Morelló, J.-R., Romero, M.-P., and Motilva, M.-J. (2004). Effect of the maturation
380 process of the olive fruit on the phenolic fraction of drupes and oils from Arbequina,
381 Farga, and Morrut cultivars. *Journal of Agricultural and Food Chemistry*, 52, 6002-
382 6009.
383 Nenadis, N., and Tsimidou, M.Z. (2017). Perspective of vibrational spectroscopy
384 analytical methods in on-field/official control of olives and virgin olive oil. *European*
385 *Journal of Lipid Science and Technology*, 119, 1600148.
386 Ram, T., Wiesman, Z., Parmet, I., and Edan, Y. (2010). Olive oil content prediction
387 models based on image processing. *Biosystems Engineering*, 105, 221-232.
388 Ranalli, A., Tombesi, A., Ferrante, M.L., and De Mattia, G. (1998). Respiratory rate of
389 olive drupes during their ripening cycle and quality of oil extracted. *Journal of the*
390 *Science of Food and Agriculture*, 77, 359-367.
391 Salguero-Chaparro, L., Baeten, V., Fernández-Pierna, J.A., and Peña-Rodríguez, F.
392 (2013). Near infrared spectroscopy (NIRS) for on-line determination of quality
393 parameters in intact olives. *Food Chemistry*, 139, 1121–1126.
394 Soto, J.N., Martínez, S.S., Gila, D.M., Ortega, J.G., and García, J.G. (2018). Fast and
395 reliable determination of virgin olive oil quality by fruit inspection using computer
396 vision. *Sensors*, 18, 3826.
397 Stella, E., Moscetti, R., Haff, R. P., Monarca, D., Cecchini, M., Contini, M., and
398 Massantini, R. (2015). Recent advances in the use of non-destructive near infrared
399 spectroscopy for intact olive fruits. *Journal of Near Infrared Spectroscopy*, 23(4), 197-
400 208.

401 Trapani, S., Migliorini, M., Cherubini, C., Cecchi, L., Canuti, V., Fia, G., and Zanoni,
402 B. (2017). Direct quantitative indices for ripening of olive oil fruits to predict harvest
403 time. *European Journal Lipid Science Technology*, 118, 1202-1212.
404 Uceda, M., and Frías, L. (1975). Epocas de recolección. Evolución del contenido graso
405 del fruto y de la composición y calidad del aceite. (Seasons of harvest. Changes on fruit
406 oil content, oil composition and oil quality). In *Proceeding of II Seminario Oleícola*
407 *Internacional; International Olive-oil Council*, Cordoba, Spain.
408 Vidal, A.M., Alcalá, S., de Torres, A., Moya, M., and Espínola, F. (2019).
409 Characterization of olive oils from superintensive crops with different ripening degree,
410 irrigation management, and cultivar: Arbequina, Koroneiki, and Arbosana. *European*
411 *Journal of Lipid Science and Technology*, 121(4), 1800360.

UNIVERSITÀ DEGLI STUDI DI MILANO
Department of Food, Environmental and Nutritional Sciences
Dipartimento di Scienze per gli Alimenti, la Nutrizione e l'Ambiente
DEFENS

Silvia Grassi
Food Science and Technology
Tel.: +39 0250319185
Fax: +39 0250319190
e-mail: silvia.grassi@unimi.it

Milan, 02 November 2020

Dear Editor,

Please, find attached all the required documents of the revised version of the manuscript " Prediction of olive ripening degree combining image analysis and FT-NIR spectroscopy for virgin olive oil optimisation" by C. Alamprese, S. Grassi, A. Tugnolo, E. Casiraghi.

All the queries of the reviewers have been properly answered in the attached "response to reviewers" letter. The changes made in the original text (and in the figures) have been properly highlighted in red in the corrected version.

We hope you could appreciate our revision work, thus reconsidering your decision.

The work described has not been published previously, is not under consideration for publication elsewhere, and its publication is approved by all authors and tacitly or explicitly by the responsible authorities where the work was carried out; if accepted, it will not be published elsewhere in the same form, in English or in any other language, including electronically without the written consent of the copyright-holder.

Please, do not hesitate to contact me for further information.

Best regards,

Silvia Grassi

Dear Editor,

first of all, we would like to thank you for the positive evaluation of our manuscript.

The manuscript was carefully revised. All the comments have been answered and changes to the manuscript have been highlighted in red throughout the text. Reviewers' comments have been very helpful to increase the quality of the manuscript.

Reviewers' comments:

Reviewer #1

The manuscript shows the use of spectroscopic data and image analysis techniques to determine the degree of ripening of olives, and the classification by using the spectral data. Actually, the degree of ripening has been commonly determined by the methodology based on physical observations of certain number of olives (MI). It is a practical and fast way to see maturity level of olives, even on site.

Now, this proposed methodology uses FT-NIR spectra of olives, analyzing the data by statistical models. The spectroscopic data were combined by image analysis to discriminate (classify) olives based on their ripening level (IA as the reference). The study uses a good number of samples, enough to calibrate, and then validated with independent sets.
The methodology proposed here does not seem practical. However, it is a new point of view, in that it shows the use of spectroscopic and IA measurements together. The experiments were designed thoroughly. It was written clearly.

We would like to thank the Reviewer for her/his generally positive evaluation of the manuscript.

Here are some questions/suggestions:

1. Lines 150-154: In the discriminant analysis, the calibration set was chosen from 2017 harvest year data. The validation set was set totally with 2016 and 2018 data. Why do the authors use calibration and validation sets from different years? Why did not they use randomly chosen sets among three-year data for both purposes.

Certainly there are different reliable strategies to split a dataset into calibration and validation sets (Oliveri, 2017). Uniform sampling designs, such as Kennard-Stone algorithm, are recommended for dividing the data when there is no obvious variable, such as time, to use for splitting data (Snee, 1977). In this study, we had different harvesting years, so we decided to use the variable "time" to split our data. Being aware that the calibration set must include the whole variability to be considered (in our case the different cultivars and different sampling times/ripening degrees), we chose samples collected in 2017 for the calibration set construction. Indeed, along 2017 year all the varieties and ripening degrees were well represented, whereas samples collected in 2016 and 2018 harvestings were less abundant due to environmental and agronomic conditions. These details have been clarified by adding a new Table 1 providing relevant information about the sampling procedure (as suggested by Reviewer 2).

Oliveri, P. (2017). Class-modelling in food analytical chemistry: development, sampling, optimisation and validation issues–a tutorial. Analytica chimica acta, 982, 9-19.

Snee, R. D. (1977). Validation of regression models: methods and examples. Technometrics, 19(4), 415-428.

2. Can authors justify their results also by the maturity index (MI) data as reference?

Thank you for the suggestion. Comments about MI ranges of the three IA classes have been added in the text (L217-220, L288-290 and L292-296).

3. If an image/picture of FT-NIR sampling can be provided, it would be helpful for the realization of spectral data collection.

A new Figure has been added in the M&M section (Fig. 2) to show the acquisition procedure.

Reviewer #2

1. Please better define the total number of samples sued, samples per region and variety.

We would like to thank the Reviewer for the comment. A table, new Table 1, has been added to provide relevant information concerning the sampling procedure.

2. More details about the scanning protocol should be added. Any effect of the olive surface, colour patterns. This must be added and discussed in the ms.

If the Reviewer refers to the FT-NIR protocol, the olive colour has no effect on the scanned signal. Indeed, the considered range (10500 - 4000 cm^{-1}) does not include the visible region of the electromagnetic spectrum. On the other hand, the interaction between NIR radiation and olive surface has an effect, which was corrected by spectral pre-treatments (smoothing, Standard Normal Variate, and first derivative). The acquisition procedure is reported in the text (L135-140). A further detail has been included in L88-94 and an image of the acquisition procedure has been added as suggested by Reviewer 1 (new Fig. 2).

As for the image acquisition, all the details are already reported in the text (L114-120). The procedure was developed to prevent light losses and environmental interferences. In this case, the olive side oriented to the glass of the scanner was the one analysed just for its colour pattern.

3. The criteria used to classify the samples must be added. The cut off must be added

The criterion used to assign samples to classes has been added in L158-162; no cut-off was used as we followed the "most probable approach" that assigns samples to the class in which they obtain the highest probability, regardless the probability magnitude.

Highlights

- Large olive dataset based on different origins, cv, ripening stages and crop years
- Development of an image analysis method for objective ripening class identification
- Image analysis classes used as references for PLS-DA models based on FT-NIR data
- Good global classification with high sensitivity (79%) and specificity (75%)

Declaration of interests

☒ The authors declare that they have no known competing financial interests or personal relationships that could have appeared to influence the work reported in this paper.

☐The authors declare the following financial interests/personal relationships which may be considered as potential competing interests:

Author contributions

Cristina Alamprese: Conceptualization, Methodology, Supervision, Writing - Original Draft.

Silvia Grassi: Conceptualization, Methodology, Software, Formal analysis, Data Curation, Writing-Original draft preparation.

Alessio Tugnolo: Formal analysis, Data curation.

Ernestina Casiraghi: Conceptualization, Supervision, Project administration, Funding acquisition.

Figure captions

Figure 1. Example of an olive image before (left) and after (right) the segmentation by using the Superpixel algorithm.

Figure 2. Image of the FT-NIR spectrometer (MPA, Bruker Optics, Milan, Italy) equipped with an integrating sphere used for the spectral data collection. The detail shows the glass Petri dish containing an olive aliquot under analysis.

Figure 3. FT-NIR spectra of olives at different ripening stages, identified according to the image analysis maturity class (class 1, green line; class 2, red line; class 3, blue): a) raw spectra; b) reduced spectra after smoothing and first derivative transformation.

Figure 4. Principal Component Analysis results of the FT-NIR spectra of olives at different ripening stages after smoothing and first derivative: a) score plot with sample identification according to the image analysis maturity classes (dark gray, class 1; light gray, class 2; black, class 3); b) score plot with sample identification according to the origin (reversed triangle, Abruzzo region; square, Calabria region; diamond, Apulia region; triangle, Sardinia region); c) loading plot (black line, PC1; grey line, PC2).

Figure 1

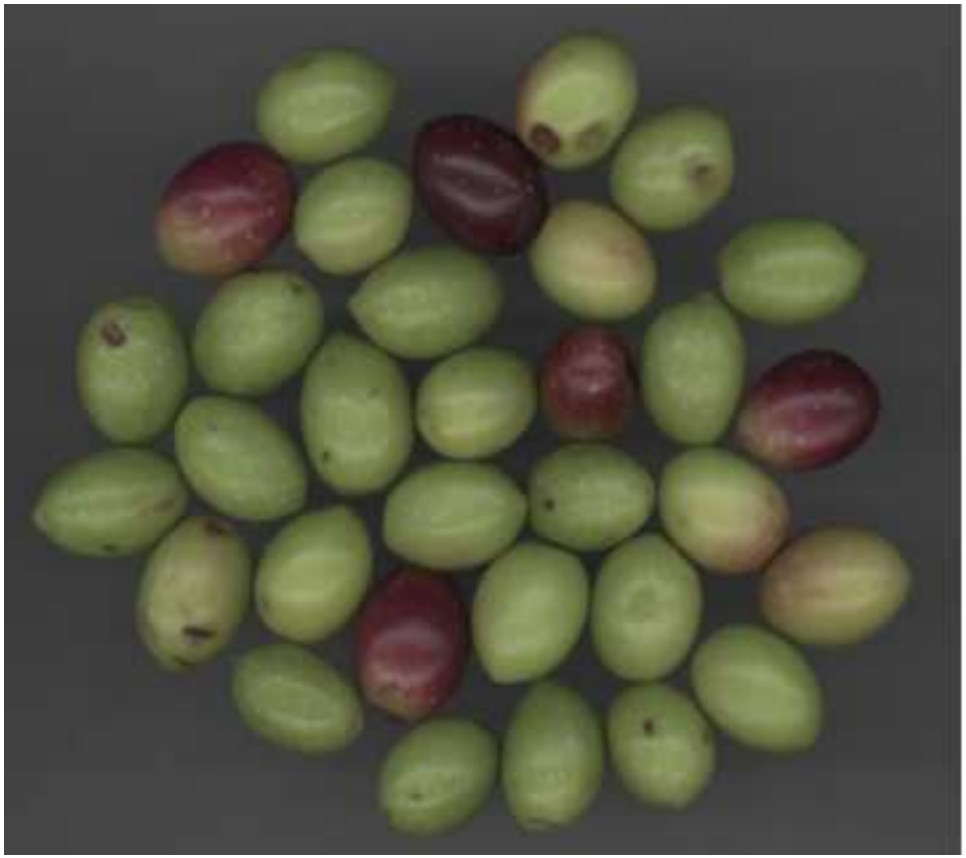

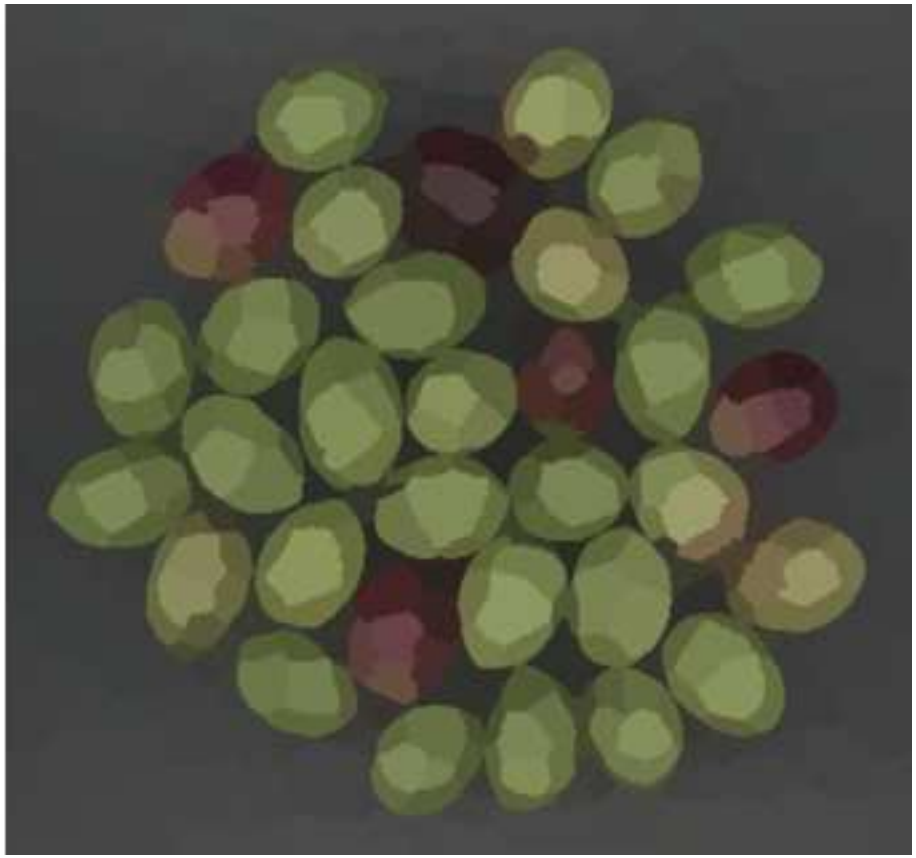

Figure 2

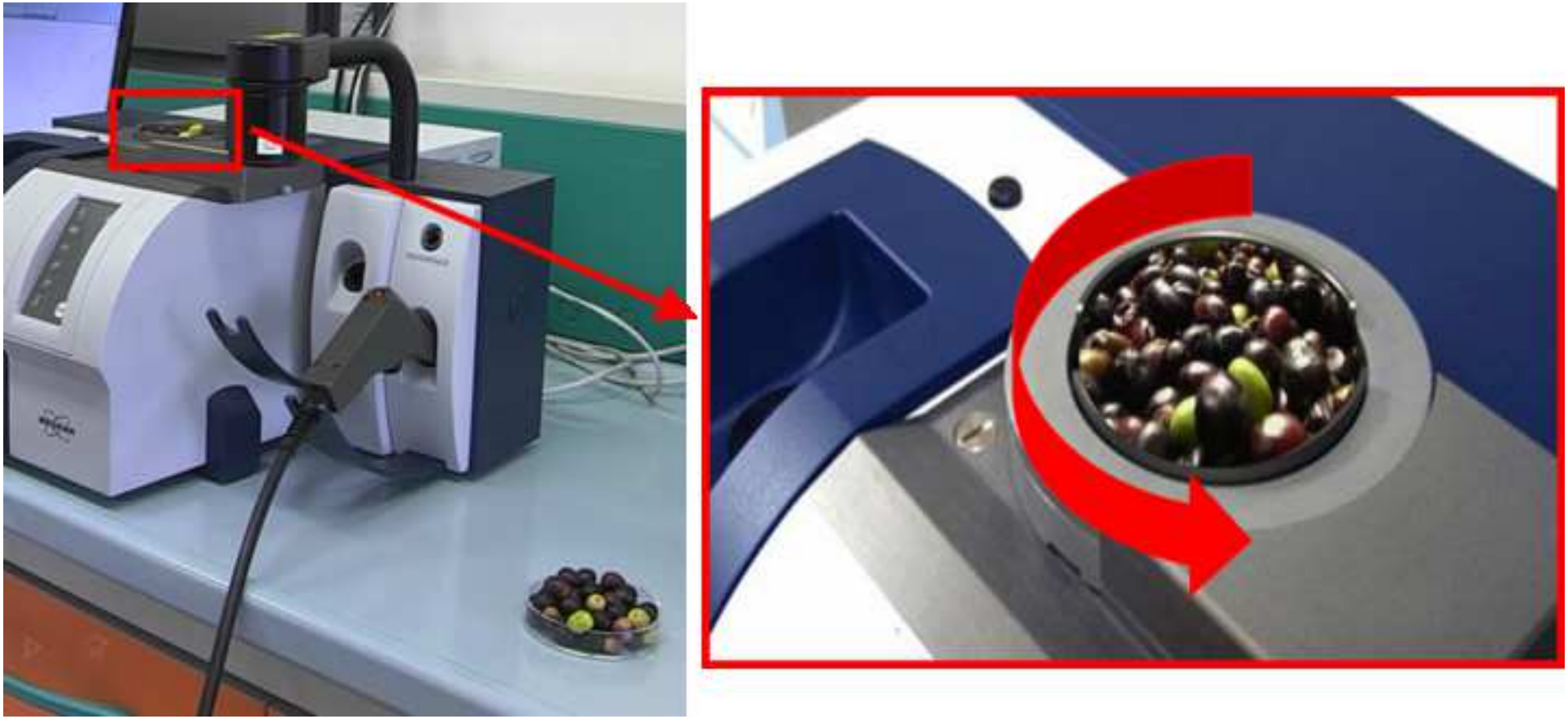

Figure 3

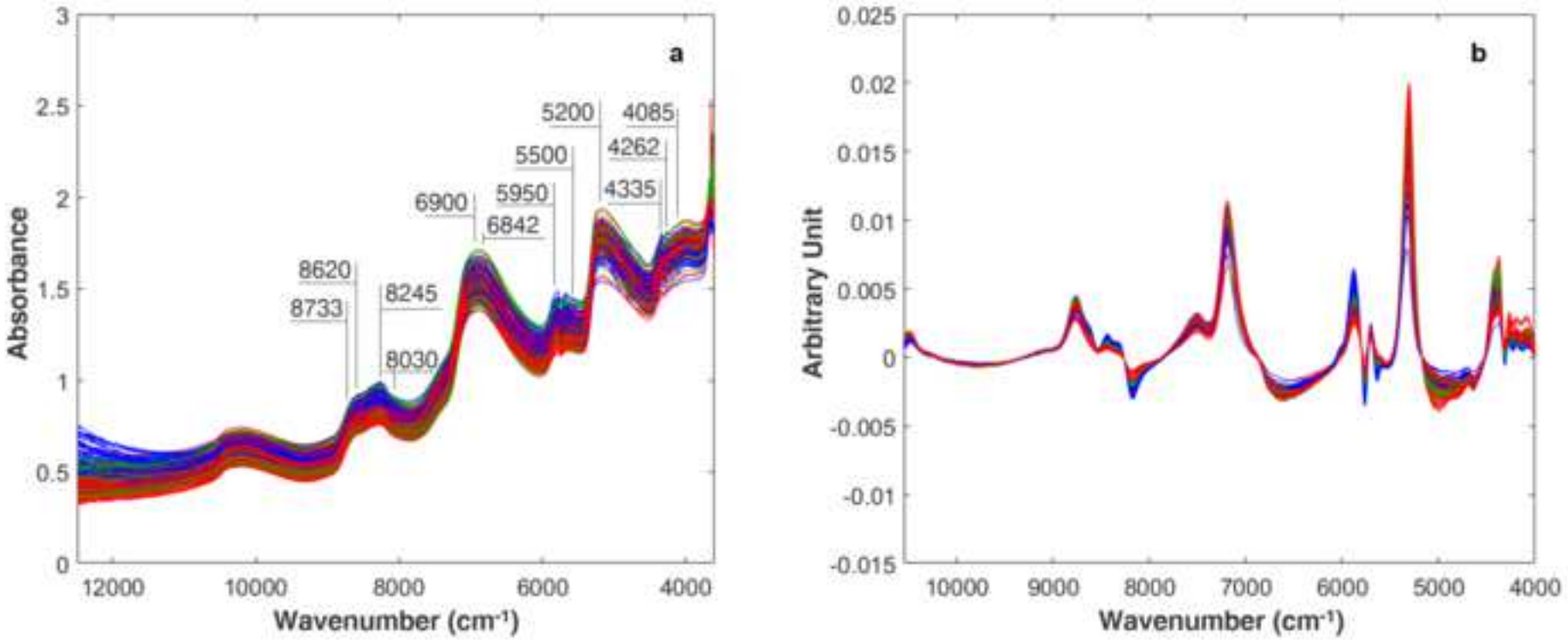
a
Absorbance
Wavenumber (cm⁻¹)
8620
8733
8245
8030
6900
6842
5950
5500
5200
4335
4262
4085
b
Arbitrary Unit
Wavenumber (cm⁻¹)

Figure 4

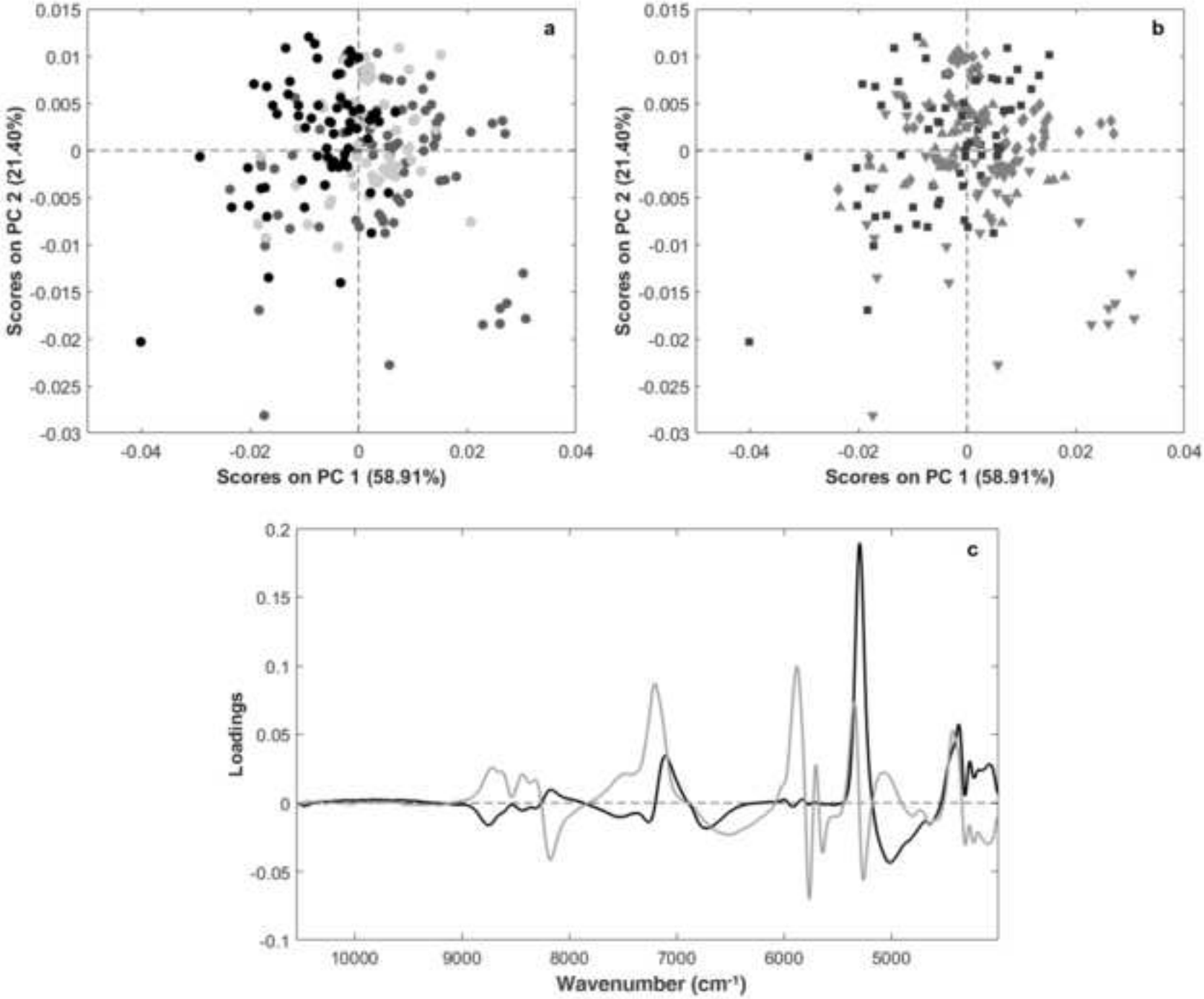
a
b
c
Scores on PC 2 (21.40%)
Scores on PC 1 (58.91%)
Loadings
Wavenumber (cm-1)
0.015
0.01
0.005
0
-0.005
-0.01
-0.015
-0.02
-0.025
-0.03
-0.04
-0.02
0
0.02
0.04
0.2
0.15
0.1
0.05
-0.05
-0.1
10000
9000
8000
7000
6000
5000

Table 1

Table 1. Overview of the olive sampling plan. T1-T5 represent the different sampling times over the ripening period.

		Sampling times per harvesting year			
Region	**Cultivar**	**2016**	**2017**	**2018**	**Number of aliquots**
Abruzzo (AR)	Dritta		T1-T2-T3-T4		23
	Gentile		T1-T2-T3-T4	T1-T2-T3	25
	Tortiglione		T1-T2-T3-T4	T1-T2	29
Calabria (CR)	Calipa		T1-T2-T3-T4-T5	T1-T2-T3-T4-T5	26
	Cannavà		T1-T2-T3-T4-T5	T1-T2-T3-T4-T5	19
	Ciciariello		T1-T2-T3-T4-T5	T1-T2-T3	23
	Filogaso		T1-T2-T3-T4-T5		21
Apulia (PR)	Bambina		T1-T2-T3	T1-T2-T3	28
	Cima di Melfi	T1-T2-T3	T1-T2-T3	T1-T2-T3	32
	Oliva Rossa	T1-T2	T1-T2-T3	T1-T2	15
Sardinia (SR)	Corsicana	T1-T2-T3-T4	T1-T2-T3-T4	T1	20
	Semidana	T1-T2-T3-T4	T1-T2-T3-T4	T1	22
	Sivigliana	T1-T2-T3-T4	T1-T2-T3-T4	T1	20

Table 2. Olive maturity classes considered in the Surface Colorimetric Index (SCI)

Class number	Olive skin colour
1	100% green
2	<50% turning red, purple or black
3	>50% turning red, purple or black
4	100% purple or black

Table 3. Olive maturity classes defined according to the red channel average intensity calculated with the developed image analysis procedure.

Class number	Olive skin colour	Red channel average intensity
1	100% green	250.0 – 90.0
2	<50% turning red, purple or black	89.9 – 71.0
3	>50% turning red, purple or black	70.9 – 0.0

Table 4. Figures of merit of PLS-DA models developed for olive maturity class prediction based on FT-NIR spectral data after smoothing and first derivative of all the olives (Global) or of the olives coming from Abruzzo Region (AR), Calabria Region (CA), Apulia Region (PR) and Sardinia Region (SR): number of Latent Variables (LV), number of samples used to calibrate the model (N-Cal) and to validate the model (N-Pred), calibration, cross-validation (CV) and prediction results in terms of sensitivity (SENS) and specificity (SPEC) percentages.

Dataset		Class 1		Class 2		Class 3		Average prediction	
		SENS	**SPEC**	**SENS**	**SPEC**	**SENS**	**SPEC**	**SENS**	**SPEC**
Global (7 LV)	**N-Cal**	*78*		*61*		*67*		*206*	
	Calibration	86	84	66	61	92	87	82	78
	CV	83	83	66	57	90	85	80	76
	N-Pred	*41*		*28*		*28*		*97*	
	Prediction	85	67	64	72	86	84	**79**	**75**
AR (5 LV)	**N-Cal**	*12*		*22*		*19*		*53*	
	Calibration	100	100	86	77	95	97	92	90
	CV	100	100	77	77	95	85	89	85
	N-Pred	*8*		*9*		*7*		*24*	
	Prediction	100	94	67	80	100	94	**87**	**89**
CR (5 LV)	**N-Cal**	*27*		*17*		*20*		*64*	
	Calibration	100	100	100	96	100	100	100	99
	CV	89	89	71	85	95	100	86	91
	N-Pred	*10*		*6*		*9*		*25*	
	Prediction	100	60	67	95	78	100	**84**	**83**
PR (4 LV)	**N-Cal**	*23*		*14*		*10*		*47*	
	Calibration	74	8	79	64	80	76	77	76
	CV	74	75	64	64	80	76	72	72
	N-Pred	*16*		*7*		*5*		*28*	
	Prediction	81	92	86	62	80	74	**82**	**81**
SR (4 LV)	**N-Cal**	*16*		*8*		*18*		*42*	
	Calibration	94	100	75	59	100	79	93	83
	CV	94	100	62	56	100	79	90	83
	N-Pred	*7*		*6*		*7*		*20*	
	Prediction	100	61	33	50	86	92	**75**	**69**